

Targeted Transgenic Expression of an Osteoclastic Transmembrane Protein-tyrosine Phosphatase in Cells of Osteoclastic Lineage Increases Bone Resorption and Bone Loss in Male Young Adult Mice*

Received for publication, October 30, 2008, and in revised form, February 24, 2009. Published, JBC Papers in Press, February 25, 2009, DOI 10.1074/jbc.M808324200

Matilda H.-C. Sheng^{‡§1}, Mehran Amoui^{‡§1}, Virginia Stiffel[‡], Apurva K. Srivastava^{‡§}, Jon E. Wergedal^{‡§}, and K.-H. William Lau^{‡§2}

From the [‡]Musculoskeletal Disease Center, Jerry L. Pettis Memorial Veterans Affairs Medical Center, Loma Linda, California 92357 and the [§]Department of Medicine, Loma Linda University, Loma Linda, California 92354

This study evaluated whether transgenic expression of PTP-oc (osteoclastic transmembrane protein-tyrosine phosphatase) in cells of the osteoclast lineage would affect bone resorption and bone density in young adult mice. Transgenic mice were generated with a transgenic construct using a tartrate-resistant acid phosphatase exon 1C promoter to drive expression of rabbit *PTP-oc* in osteoclastic cells. pQCT evaluation of femurs of young adult male progeny of three lines showed that transgenic mice had reduced bone volume and area, cortical and trabecular bone mineral content, and density. Histomorphometric analyses at secondary spongiosa of the femur and at metaphysis of the L4 vertebra confirmed that male transgenic mice had decreased trabecular surface, reduced percentage of trabecular area, decreased trabecular number, increased trabecular separation, and increased osteoclast number per bone surface length. Consistent with an increase in bone resorption, the serum C-telopeptide level was 25% higher in transgenic mice than in wild-type littermates. However, the bone phenotype was not readily observed in female young adult transgenic mice. This could in part be due to potential interactions between estrogen and PTP-oc signaling, since the bone loss phenotype was seen in young adult ovariectomized transgenic mice by microcomputed tomography analysis. *In vitro*, the average pit area per resorption pit created by marrow-derived transgenic osteoclasts was ~50% greater than that created by wild-type osteoclasts. Transgenic osteoclasts showed a lower *c-Src* phosphotyrosine 527 level, greater *c-Src* kinase activity, and increased tyrosine phosphorylation of paxillin. In summary, this study provides compelling *in vivo* evidence that PTP-oc is a positive regulator of osteoclasts.

There is ample evidence that reversible protein tyrosine phosphorylation is an important regulatory mechanism in

determining overall functional activity of mature osteoclasts. Although the roles of several cellular protein-tyrosine kinases (PTKs),³ such as *c-Src* PTK, in regulating osteoclast activity have been documented (1–3), little is known about the identity of protein-tyrosine phosphatases (PTPs) involved in the regulation of osteoclast activity. In this regard, our laboratory had previously cloned from a rabbit osteoclast cDNA library a full-length cDNA of a structurally unique transmembrane PTP, which we termed osteoclastic PTP, *PTP-oc* (4). *PTP-oc* is found to be expressed predominantly in hematopoietic cells of monocyte-macrophage lineage, mature osteoclasts, and B-lymphocytes (4, 5). Unlike most transmembrane PTPs, it has a very short (8 residues) extracellular domain, lacks a signal peptide, contains only a single PTP catalytic domain, and is relatively small (405 residues). *PTP-oc* shares the gene structure of a renal receptor-like PTP, termed *Glepp1* (glomerular epithelial protein 1) (also known as *PTP-U2*, *PTPRO*, *PTP-ϕ*, *CRYP2*, or *PTP-BK*) (6–8) on human chromosome 12p12–p13 (6) or mouse chromosome 6 (9). With the exception of a 28-amino acid insert at the cytosolic juxtamembrane region, *PTP-oc* shows complete sequence identity with the transmembrane and intracellular domains of *Glepp1* (4). Thus, *PTP-oc* is also referred to as *PTP-U2S* or *PTPROt*. *PTP-oc* is not an alternative splicing variant of *Glepp1*, and its expression is driven by an alternative, cell type-specific, intronic promoter (10–12). The basal elements of the intronic promoter of murine *PTP-oc* have recently been characterized and compared with that of the human *PTP-oc* gene (12).

Our *in vitro* studies have accumulated a large body of strong evidence that PTP-oc may function as a positive regulator of osteoclast activity and that its molecular mechanism is in part mediated through activation of *c-Src* PTK by dephosphorylating its inhibitory Tyr(P)⁵²⁷ residue. Accordingly, suppression of *PTP-oc* expression in rabbit osteoclasts by a *PTP-oc* antisense oligodeoxynucleotide reduced their bone resorption activity,

* This work was supported in part by a Veterans Affairs Merit Review grant and by a special appropriation to the Jerry L. Pettis Memorial Veterans Affairs Medical Center, Musculoskeletal Disease Center. Preliminary results were presented in abstract form (43).

¹ Both authors contributed equally to this work.

² To whom correspondence should be addressed: Musculoskeletal Disease Center (151), Jerry L. Pettis Memorial VA Medical Center, 11201 Benton St., Loma Linda, CA 92357. Fax: 909-796-1680; E-mail: William.Lau@med.va.gov.

³ The abbreviations used are: PTK, protein-tyrosine kinase; BMC, bone mineral content; BMD, bone mineral density; *C_T*, critical cycle threshold; m-CSF, macrophage colony-stimulating factor; pQCT, peripheral quantitative computed tomography; PTP, protein-tyrosine phosphatase; RT, reverse transcription; sRANKL, soluble receptor activator of NF-κB ligand; SV40(A)_{LT}, SV40 late poly(A) signal; Tb, trabecular; WT, wild-type; μ-CT, microcomputed tomography; OVX, ovariectomized; BV, bone volume; TV, tissue volume; ERα, estrogen receptor α.

Transgenic Expression of PTP-oc Increased Bone Resorption in Mice

which was accompanied by an increase in Tyr(P)⁵²⁷ level of c-Src (13). Osteoclast-like cells derived from U937 cells (14) or RAW264.7 cells (15) overexpressing wild-type (WT) *PTP-oc* produced larger and deeper resorption pits than those derived from control cells, whereas osteoclast-like cells derived from U937 cells or RAW264.7 cells expressing the phosphatase-deficient *PTP-oc* mutant (15) yielded smaller and shallower pits *in vitro*. Overexpression of WT *PTP-oc* activated and transgenic expression of the phosphatase-deficient *PTP-oc* mutant or treatment with *PTP-oc* small interfering RNA inhibited the c-Src signaling pathway in these cells (14, 15). Up-regulation of *PTP-oc* expression by certain resorption activators in rabbit osteoclasts resulted in dephosphorylation of Tyr(P)⁵²⁷ of c-Src, and cellular PTP-oc levels correlated strongly with c-Src PTK activation (16). In addition, the c-Src Tyr(P)⁵²⁷ peptide was shown to be a good substrate for recombinant rabbit PTP-oc *in vitro* (16).

In this study, we sought to generate transgenic mice with targeted overexpression of *PTP-oc* in cells of osteoclast lineage and to determine their bone phenotype in order to assess whether PTP-oc indeed has a regulatory role in the bone resorption activity of osteoclasts *in vivo*. We chose a targeted transgenic overexpression strategy over the general overexpression approach to avoid potential confounding effects of *PTP-oc* overexpression in other organs or tissues, particularly the kidney, since *Glepp1* (which has the identical intracellular and catalytic domains as *PTP-oc*) has important regulatory functions in the kidney (17). The kidney is one of the key extraskeletal organs that regulate bone and mineral metabolism. Overexpression of *PTP-oc* in the kidney may yield confounding results with respect to bone and mineral metabolism. To target expressing *PTP-oc* in cells of osteoclast lineage, we used *TRACP* (tartrate-resistant acid phosphatase) exon 1C promoter to drive *PTP-oc* expression. Among the known *TRACP* promoters, the exon 1C promoter appeared to be the most specific for osteoclastic cells (18). Also, *TRACP* exon 1C promoter is a weak promoter *in vivo* (19). We reasoned that the use of a weak but highly specific promoter would allow for specific *PTP-oc* overexpression in cells of osteoclast lineage but at the same time may avoid the too high levels of transgene expression that could yield off-target effects.

EXPERIMENTAL PROCEDURES

Materials—Tissue culture plasticware was obtained from Falcon (Oxnard, CA). Minimum essential medium α was from Invitrogen. Fetal bovine serum was purchased from HyClone (Logan, UT). The pGL3-TRACP-1C-*Luc* plasmid (18) was generously provided by Dr. A. Ian Cassady of the University of Queensland in Australia. The enhanced chemiluminescence detection kit was obtained from Pierce. X-ray films were obtained through local suppliers. Immobilon-P transfer membrane was a product of Millipore (Bedford, MA). A specific polyclonal anti-PTP-oc antibody against the N-terminal fragment of the rabbit PTP-oc was generated in guinea pigs as described previously (13). Anti-Tyr(P)⁵²⁷ c-Src, anti-c-Src, anti-paxillin, and anti-Tyr(P)-paxillin antibodies were purchased from Upstate Biotechnology, Inc. (Lake Placid, NY), Santa Cruz Biotechnology, Inc. (Santa Cruz, CA), or BD Trans-

duction Laboratories (San Diego, CA). PP2 was a product of Calbiochem. Other chemicals were from Thermo-Fisher (Los Angeles, CA) or Sigma.

Construction of pGL3-TRACP-1C-PTP-oc Plasmid—Briefly, the luciferase (*Luc*) gene of the pGL3-TRACP-1C-*Luc* plasmid was excised at NcoI and XbaI sites. The NcoI and XbaI restriction sites were added by PCR in frame to the 5'- and 3'-end of the full-length rabbit *PTP-oc* cDNA, respectively. The purified NcoI- and XbaI-digested pGL3-TRACP-1C plasmid was then ligated with the NcoI and XbaI restriction sites-added rabbit *PTP-oc*, forming the pGL3-TRACP-1C-*PTP-oc* plasmid (Fig. 1). The sequence and orientation of the pGL3-TRACP-1C-*PTP-oc* expression plasmid was confirmed by DNA sequencing.

In Vitro Analyses of Cell Type Specificity of the pGL3-TRACP-1C-PTP-oc Expression Plasmid—Briefly, osteoclastic (murine RAW264.7 cells) and nonosteoclastic cells (murine MC3T3-E1, human TE85 osteosarcoma cells, human HepG2 hepatic cells, and human HEK293 kidney cells) were each plated in quadruplicate for 24 h at 5×10^4 cells/well in 24-well plates. 0.2 μ g each of the pGL3-TRACP-1C-*PTP-oc* or pGL3-TRACP-1C-empty plasmid (negative control) DNA was transiently transfected into each cell type with the Effectene transfection reagent (Qiagen, Valencia, CA). To adjust for the vastly different transfection efficiencies among these cell types, parallel cell cultures were transfected with the pGL3-control plasmid, which contains the *SV40* promoter to drive *Luc* expression. Relative *PTP-oc* mRNA levels in each cell type, normalized against the luciferase activity of corresponding pGL3-control-transfected cells, were determined to assess cell type specificity of the *TRACP* exon 1C promoter.

To measure relative *PTP-oc* mRNA levels, total RNA was isolated using the RNeasy minikit (Qiagen) 2 days after the transfection. Each DNase I-treated RNA sample (1 μ g) was reverse-transcribed to cDNA using the ThermoScriptTM reverse transcription-PCR system (Invitrogen). The relative mRNA levels of rabbit *PTP-oc* and the β -actin housekeeping gene were quantified by real time PCR using the following primer sets: for rabbit *PTP-oc*, forward primer (5'-GTC TGC TGC TTG TTA CTC TC-3') and reverse primer (5'-GCA TCT CAT CAG CGT AGT TG-3'); for β -actin: forward primer (5'-CCA TGT ACG TGG CCA TCC AG-3') and reverse primer (5'-AAG CGC TCG TTG CCG ATG GT-3'). The PCR reaction was performed with the QuantiTect SYBR Green PCR kit (Qiagen) in an MJ Research DNA Engine Opticon 2 machine, under a condition of 10-min hot start at 95 °C, followed by 40 cycles of 95 °C for 30 s, 54 °C for 30 s, and 72 °C for 45 s. The reaction was ended with 10 min at 72 °C. The relative level of *PTP-oc* mRNA was determined by the critical cycle threshold (ΔC_T) method: C_T of *PTP-oc* - C_T of β -actin. To assess relative transfection efficiency, The luciferase activity in cell extracts of parallel pGL3-control-transfected cultures was determined using a commercial assay kit (Promega, Madison, WI) with a luminometer (model 3010; Analytical Scientific Instruments, Richmond, CA).

Production of Transgenic Mice with Targeted PTP-oc Overexpression in Cells of Osteoclast Lineage—All animal protocols were approved by the Animal Care and Use Committee of the Jerry L. Pettis Memorial Veterans Affairs Medical Center.

Transgenic founder mice were generated by the Transgenic Core Facility of the Norris Comprehensive Cancer Center of the University of Southern California (Los Angeles, CA). Because it was necessary to remove the backbone structure of the pGL3 vector prior to its injection into fertilized ova, the TRACP-1C-PTP-oc fragment, including the SV40 late poly(A) signal (SV40(A)_n) was excised from the pGL3-TRACP-1C-PTP-oc plasmid by SacI and BamHI restriction enzyme treatments. The internal BamHI site within rabbit PTP-oc cDNA was mutated without altering its primary amino acid sequence using a PCR-based site-directed mutagenesis kit (Stratagene, La Jolla, CA) prior to the restriction enzyme treatment. The purified TRACP-1C-PTP-oc-SV40(A)_n fragment was then microinjected into the pronucleus of fertilized B6D2F1 ova, which were then implanted into pseudopregnant foster mothers. After weaning, the pups were transferred to the Animal Research Facility of the Jerry L. Pettis Memorial Veterans Affairs Medical Center. PTP-oc transgenic mice were identified with a PCR-based genotyping assay (see below). The transgenic founder mice, which have a 50% C57BL/6J and 50% DBA2 genetic background, were mated with WT C57BL/6J mice of the opposite sex to produce F1 progenies. The F1 progenies were intercrossed to yield F2 progenies, which were used in the study along with corresponding WT littermates. In some experiments, the F2 transgenic progenies were backcrossed with C57BL/6J mice for six generations to yield transgenic mice with >99.6% C57BL/6J genetic background.

Genotyping Assay—Tail vertebrate tissue (1 cm) was taken from each pup at weaning and digested overnight at 55 °C in 330 μl of the ATL tissue lysis buffer (Qiagen) supplemented with 10% proteinase K. Genomic DNA was purified using Qiagen DNeasy tissue minicolumns. The quality and quantity of the genomic DNA were analyzed by measuring the absorbance ratio of 260 nm/280 nm. A PCR-based genotyping method was set up to identify transgenic mice using a forward primer corresponding to a unique region upstream to the 5′-end of the TRACP-1C promoter (5′-GTT GGT GGT GAG TGT TCA AGG AAG GAG TCT-3′) and a reverse primer corresponding to a unique region downstream to the 3′-end of the rabbit PTP-oc gene (5′-ACT GCT CCT CTG TCT GTA CCA TAG ACA TCC-3′). The PCR condition included a 5-min hot start at 95 °C and 35 cycles of amplification, each consisting of 1 min at 94 °C, 1 min at 61.5 °C, and 4 min at 70 °C. This was then followed by a final 10 min at 72 °C. The PCR product was analyzed by agarose gel electrophoresis. Genomic DNA of transgenic mice yielded a single 3.2-kb PCR band.

Peripheral Quantitative Computed Tomography (pQCT)—pQCT scanning of the femur was performed as previously described (20) using a Stratec XCT 960 M pQCT (Norland Medical Systems, Madison, WI). Briefly, femurs were fixed in 10% formalin for 24 h and stored in cold phosphate-buffered saline supplemented with 0.1% NaN₃ until measurement. The length of each femur was determined with a digital caliper. The distance between individual scanning slices was calculated by the expression, (bone length × 11)/100. The entire femur was scanned to generate values for nine consecutive slices. The derived values of slice 2 or slice 5 represented measurements at the primary/secondary spongiosa or midshaft, respectively.

Trabecular bone mineral content (BMC) and bone mineral density (BMD) were determined with the threshold setting of 230–630 mg/cm². A threshold setting of 630 mg/cm² was used to determine cortical bone parameters. These pQCT settings for corresponding bone parameters have previously been validated by bone histomorphometry (20).

Microcomputed Tomography (μ-CT) Measurements of Young Adult Ovariectomized (OVX) Mice—Groups of five 8-week-old female transgenic mice or age-matched female WT littermates were subjected to OVX or sham operation. All animals were euthanized 4 weeks after the surgery at 12 weeks of age. The bone phenotype was assessed on the right femur by μ-CT using a Scanco vivaCT40 μ-CT scanner (Scanco Medical, Brüttisellen, Switzerland). Trabecular measurements were performed at the secondary spongiosa of the distal femur (for trabecular bone). Briefly, the femur was placed in a 1.7-ml Eppendorf tube and was scanned using high resolution (55,000 V with an intensity of 145 μA). Thirty-six slices (360 μm) distal from the bottom of the growth plate were excluded to avoid the entire primary spongiosa. The trabecular bone at the secondary spongiosa was scanned at 10-μm slices at 10-μm increments to cover a total distance of 1.8 mm. The scanned image was then contoured to exclude cortical bone and focused only on trabecular bone. The slices were analyzed using the threshold setting of 230–1,000 mg/cm³. Cortical bone parameters were performed at the midshaft of the femurs, and the 1-mm midshaft of the formalin-fixed femur was scanned using high resolution (70,000 V with an intensity of 114 μA). Fifty slices (at 10-μm increments) from each side of the center of the bone were scanned (a total of 100 slices) and analyzed using a threshold setting of 260–1,000 mg/cm³. Bone parameters were calculated using the analytical tool software of Scanco.

Histomorphometry—Bone histomorphometry of femurs or the L4 lumbar vertebra of 10-week-old transgenic mice and WT littermates was determined as previously described (21). Briefly, demineralized femurs or L4 lumbar vertebra were embedded in paraffin or glycolmethacrylate. Serial longitudinal sections (5 μm in thickness) were stained for TRACP to identify osteoclasts. Histomorphometric parameters were measured at the secondary spongiosa (0.35 mm distal to the growth plate) of the femur or at the metaphysis site of the L4 vertebra at a site 0.35 mm away from the edge. Total trabecular (Tb) bone surface length, Tb area, TRACP-positive bone surface, and number of osteoclasts per bone surface in the endosteum were determined using the OsteoMeasure™ system (OsteoMetrics, Decatur, GA) under a bright field microscope, as previously described (21).

To determine dynamic bone formation parameters, 7-week-old male animals were injected with demeclocycline (25 mg/kg body weight, intraperitoneally; Sigma). A second injection with tetracycline hydrochloride (25 mg/kg body weight, intraperitoneally; Sigma) was performed 6 days later. One day after the second injection, the mice were sacrificed (*i.e.* at 8 weeks old), and femurs were removed, immediately fixed with 10% cold neutral-buffered formalin, dehydrated, and embedded into methylmethacrylate. Longitudinal sections (10 μm in thickness) were prepared. Length of single and double tetracycline labels and width of dual labels were measured at the secondary

Transgenic Expression of *PTP-oc* Increased Bone Resorption in Mice

spongiosa (0.35 mm distal from the bottom edge of the growth plate) with a total measurement area of up to 1.2 mm² per specimen, using the OsteoMeasureTM system under a fluorescent microscope. Bone formation rate and mineral apposition rate were then calculated.

Blood and Serum Assays—Blood samples were obtained from each mouse through retro-orbital veins. Serum levels of C-telopeptide of type I collagen were analyzed with an enzyme-linked immunosorbant assay, as described previously (22). This assay is specific for C-terminal peptide fragments of mouse type-I collagen released during bone resorption. The sensitivity of the C-telopeptide enzyme-linked immunosorbant assay is <0.1 ng/ml, with an average intra- and interassay coefficient of variation of <12% (22).

Complete blood count analyses were performed with ~100 μ l of freshly drawn blood collected in EDTA-coated capillary tubes using an automatic Hemavet HT950 hematology analyzer for mice (Drew Scientific, Dallas, TX). All assays were done in duplicate, and the operator was blinded to the identity of the animal group.

Marrow-derived Osteoclast Cultures—Primary bone marrow cells were flushed out of long bones of 6–10-week-old transgenic mice and WT littermates and were cultured in minimum essential medium α containing 10% fetal bovine serum. After a 24-h culture, nonadherent marrow cells, which included osteoclast precursors, were collected and plated at a density of 4×10^5 cells/cm² in minimum essential medium α with 10% fetal bovine serum in the presence of 50 ng/ml sRANKL (Santa Cruz Biotechnology) and 50 ng/ml m-CSF (Calbiochem). Under this condition, clearly identifiable TRACP+, multinucleated osteoclasts began to appear after 3 days, and the majority of cells became large TRACP+, multinucleated osteoclasts typically after 5–7 days of the treatment.

Real Time RT-PCR Analyses for Relative Rabbit and Mouse *PTP-oc* mRNA Levels—Total RNA was isolated from marrow-derived osteoclasts from 8-week-old male *PTP-oc* transgenic mice and respective age-matched male WT littermates with the RNeasy[®] minikit (Qiagen) and was reverse-transcribed to cDNA using the ThermoScriptTM RT-PCR system. The mRNA of the rabbit *PTP-oc* transgene and that of endogenous mouse *PTP-oc* were each quantified, separately, by real time PCR and were normalized against each respective β -actin mRNA level. To distinguish rabbit *PTP-oc* mRNA from endogenous mouse *PTP-oc* mRNA, two sets of gene-specific PCR primers against the most variable regions of the rabbit and mouse *PTP-oc* cDNA sequence were designed and synthesized by Integrated DNA Technologies (Coralville, IA). The PCR primer set for the rabbit *PTP-oc* cDNA was as follows: forward primer, 5'-ATG CCG CTG AAA GTA TCC TG-3'; reverse primer, 5'-ATG ACC TCA TTT CCG ACA CC-3'. The primer set for the mouse *PTP-oc* cDNA was as follows: forward primer, 5'-GTG GCT GAG GAA GAA GCA AC-3'; reverse primer, 5'-CAG CAG GGA CTC GAT TTA GC-3'. Each PCR amplification reaction was performed for 40 cycles, consisting of denaturation at 95 °C for 15 s and annealing and extension at 60 °C for 1 min each after an initial hot start at 95 °C for 10 min. Under these conditions, the rabbit *PTP-oc* PCR primers did not anneal to the mouse *PTP-oc* cDNA template at this temperature and

vice versa (data not shown). The relative level of gene expression was determined by the C_T method. To avoid the confounding issue of potential variations in priming efficiencies of the two primer sets, a standard curve method (similar to the method used in our previous gene therapy study to distinguish exogenous human *Cox-2* mRNA from endogenous rat *Cox-2* molecule (23)) was used to estimate the number of copies of respective *PTP-oc* mRNA. A standard curve for the rabbit or mouse *PTP-oc* cDNA was each constructed by plotting respective C_T against the amount of rabbit or mouse *PTP-oc* cDNA standard. The relative -fold overexpression was determined by dividing the number of copies of rabbit *PTP-oc* mRNA by that of endogenous mouse *PTP-oc* mRNA.

Resorption Pit Formation Assay—The nonadherent marrow osteoclast precursors were plated on dentine slices at a density of $1-2.5 \times 10^5$ cells/cm² and treated with sRANKL and m-CSF for 7 days. At the end of each experiment, dentine slices were trypsinized and sonicated to remove attached osteoclasts, and resorption pits were stained with acid-hematoxylin (Sigma) for 20 min. The sizes of individual pits were measured with the OsteoMeasure system.

Western Blotting—Total cellular protein was extracted with Sigma radioimmunoprecipitation assay buffer supplemented with the Sigma protease inhibitor mixture (catalog number P8370), 1 mM phenylmethylsulfonyl fluoride, 1 mM NaF, and 2 mM Na₃VO₄. Western immunoblots for total and Tyr(P)⁵²⁷ species of c-Src were performed using primary and secondary antibodies from Santa Cruz Biotechnology and Sigma, respectively, followed by enhanced chemiluminescence.

In Vitro c-Src PTK Assay—Briefly, the c-Src protein in cell extracts of transgenic and WT marrow-derived osteoclasts were isolated by immunoprecipitation using a rabbit anti-c-Src polyclonal antibody. The PTK activity of the resuspended immunoprecipitated c-Src protein was assayed by incorporation of [³²P]phosphate into a synthetic peptide (KVEKIGEG-TYGVVYK) that corresponds to the phosphorylation site of p34^{cdc2} using a Src kinase assay kit (Millipore/Upstate Biotechnology). The assay was done at 30 °C in the presence or absence of a specific inhibitor of c-Src PTK, PP2 (10 μ M). The PP2-inhibitable PTK activity represented the c-Src PTK activity.

Statistical Analysis—The results are shown as means \pm S.E. Statistical significance was determined with the two-tailed Student's *t* test. Dosage effects of sRANKL on formation of osteoclasts were assessed with analysis of variance. The difference was significant when *p* was <0.05.

RESULTS

Generation of *PTP-oc* Transgenic Mice—Fig. 1 shows the schematic representation of our *PTP-oc* transgenic targeting expression plasmid, which employed the TRACP exon 1C promoter to drive expression of the rabbit *PTP-oc* gene. The cell type specificity of this promoter for osteoclastic cells was confirmed, *in vitro*, since the relative *PTP-oc* mRNA expression level (adjusted against transfection efficiency) was more than 3,000-fold higher in the osteoclastic precursor cell line, RAW264.7 cells, than that in nonosteoclastic cells (*i.e.* murine MC3T3-E1 cells, human TE85 cells, human HepG2 cells, and human HEK293 cells) (Fig. 2A). To generate *PTP-oc* transgenic

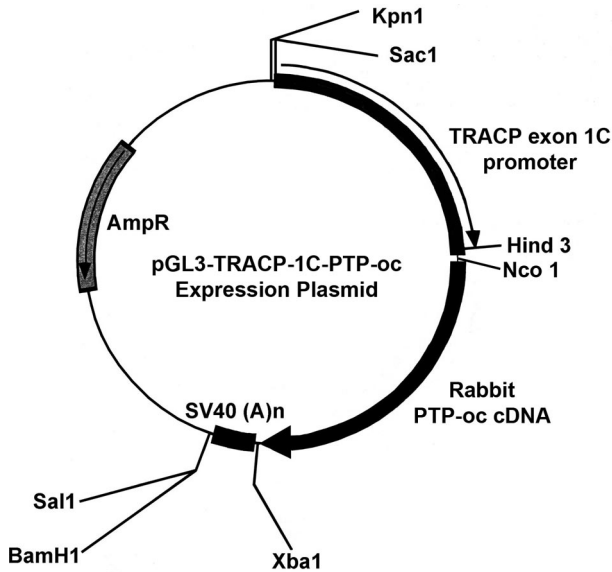


FIGURE 1. Schematic representation of the pGL3-TRACP-1C-PTP-oc expression plasmid. The construction of the pGL3-TRACP-1C-PTP-oc plasmid was prepared by cloning the full-length rabbit PTP-oc cDNA into the NcoI/XbaI site of the pGL3-TRACP-based vector (18) as described under "Experimental Procedures."

founder mice, the SacI/BamHI liberated TRACP-1C-PTP-oc-SV40(A)_n fragment of the pGL3-TRACP1C-PTP-oc plasmid was injected into the pronucleus of fertilized B6D2F1 ova, which were then implanted into pseudopregnant foster mothers. Of a total of 41 pups, six (three females and three males) were confirmed to be transgenic founders. One female founder did not produce offspring, and another female founder cannibalized all of her offspring. One transgenic line was lost during breeding. A total of three PTP-oc transgenic colonies (lines 1–3) were subsequently established.

Confirmation of PTP-oc Overexpression in Osteoclasts of Transgenic Mice—To confirm that these transgenic mice indeed overexpressed PTP-oc in osteoclasts, relative levels of the rabbit PTP-oc mRNA and those of endogenous mouse PTP-oc mRNA in marrow-derived osteoclasts of 15 young adult male F2 transgenic mice of line 1 and those in osteoclasts of 10 male age-matched WT littermates were measured by real time RT-PCR. Typical to transgenic mouse studies, there was a large variation in the levels of rabbit PTP-oc mRNA expression in marrow-derived osteoclasts of transgenic mice, ranging from 1% of to 64-fold the endogenous mouse PTP-oc mRNA levels, with an average of 4.81 ± 4.26 -fold endogenous mouse PTP-oc mRNA. The majority of transgenic osteoclasts had less than 2-fold up-regulation. The relatively low levels of PTP-oc overexpression are consistent with our prediction that use of the weak TRACP exon 1C promoter would not yield too high levels of PTP-oc overexpression in transgenic osteoclasts. We also measured the relative levels of rabbit PTP-oc mRNA (by real time RT-PCR) in several vital organs (liver, kidney, spleen, and heart) of young adult male transgenic mice compared with that in marrow-derived transgenic osteoclasts (Fig. 2B). The heart and liver of these transgenic mice did not express appreciable levels of rabbit PTP-oc mRNA, whereas marrow-derived osteoclasts of these transgenic mice expressed very high levels of

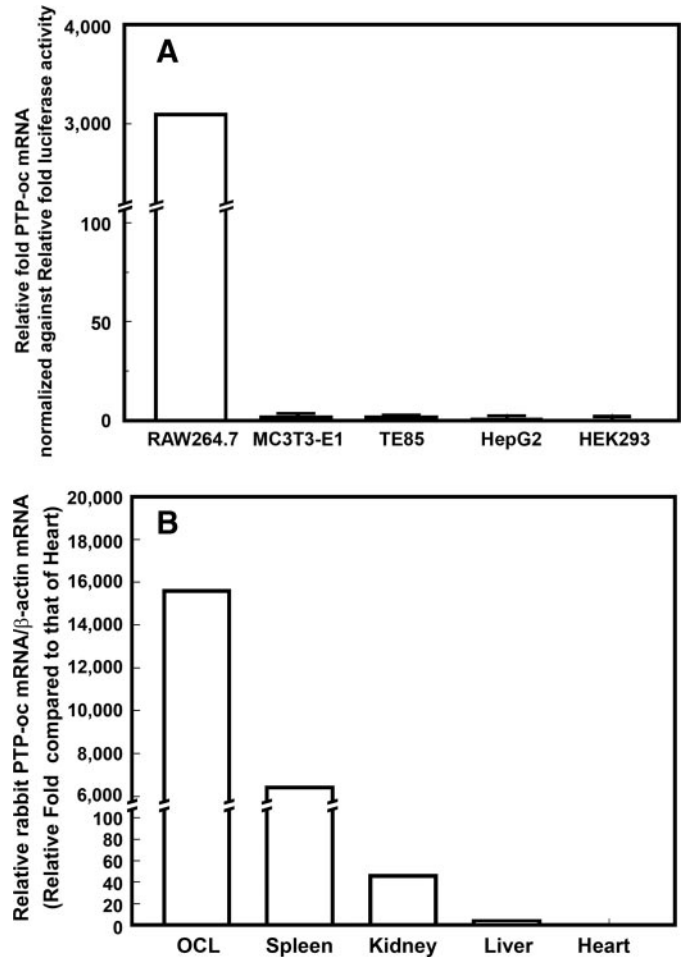


FIGURE 2. Cell type specificity of the pGL3-TRACP-1C-PTP-oc expression plasmid *in vitro* (A) and *in vivo* (B). A, an osteoclastic cell line (murine RAW264.7 monocytic cells) and four nonosteoclastic cell lines (murine MC3T3-E1 osteoblastic cells, human TE85 osteosarcoma cells, human HepG2 hepatic cells, and human HEK293 embryonic kidney cells) were transfected with pGL3-TRACP-1C-PTP-oc or pGL3-TRACP-1C empty plasmid (negative control). To determine relative transfection efficiencies in these cell lines, parallel cultures of each cell type were transfected with the pGL3-control plasmid. Relative rabbit PTP-oc mRNA levels and luciferase activity in each transfected cell cultures were determined as described under "Experimental Procedures." To adjust for the vast differences in transfection efficiencies, the results are shown as relative -fold PTP-oc mRNA levels per luciferase activity (mean \pm S.E. $n = 4$). None of the cell lines transfected with the pGL3-TRACP-1C empty plasmid showed detectable rabbit PTP-oc mRNA levels. B, total RNA was isolated from marrow-derived osteoclasts (OCL) and the spleen, kidney, liver, and heart of young adult male transgenic mice. Relative rabbit PTP-oc expression levels (normalized against respective β -actin mRNA levels) were determined by real time RT-PCR in triplicate as described under "Experimental Procedures." Results are shown as the mean of relative -fold level of the normalized PTP-oc mRNA levels in the heart (*i.e.* the adjusted rabbit PTP-oc mRNA in hearts of transgenic mice was set as 1-fold).

rabbit PTP-oc mRNA levels (15,650-fold that in hearts of transgenic mice). Their kidneys also had very low levels of rabbit PTP-oc mRNA ($\sim 0.3\%$ of the levels in transgenic osteoclasts). However, their spleens expressed high levels of rabbit PTP-oc mRNA ($\sim 40\%$ of that of osteoclasts). This is not unexpected, since the spleen is a major extramedullary source of hematopoietic cells, which include TRACP exon 1C-expressing osteoclast precursors. These findings confirm the *in vivo* tissue specificity of the TRACP exon 1C promoter for osteoclastic cells.

Transgenic Expression of *PTP-oc* Increased Bone Resorption in Mice

TABLE 1

Comparison of bone phenotype of 10-week-old male mice from three transgenic lines (TG) with targeted *PTP-oc* overexpression in cells of osteoclastic lineage with corresponding age- and sex-matched WT littermates (mean \pm S.E.)

	Transgenic line 1		Transgenic line 2		Transgenic line 3	
	WT (<i>n</i> = 7)	TG (<i>n</i> = 11)	WT (<i>n</i> = 8)	TG (<i>n</i> = 8)	WT (<i>n</i> = 13)	TG (<i>n</i> = 14)
Body weight (g)	28.6 \pm 0.9	25.1 \pm 0.5 ^a	25.6 \pm .8	22.1 \pm .7 ^b	24.7 \pm 0.7	23.2 \pm 0.5
Bone length (mm)	15.1 \pm 0.1	14.7 \pm 0.2 ^c	14.7 \pm 0.2	14.2 \pm 0.2 ^c	15.0 \pm 0.1	14.5 \pm 0.1 ^a
Bone volume (mm ³)	3.00 \pm 0.08	2.71 \pm 0.09 ^b	2.67 \pm .09	2.26 \pm 0.08 ^a	3.00 \pm 0.07	2.64 \pm 0.06 ^d
Total bone area (mm ²)	1.80 \pm 0.03	1.68 \pm 0.05 ^c	1.67 \pm .05	1.44 \pm 0.03 ^a	1.82 \pm 0.03	1.66 \pm 0.03 ^a
Medullary area (mm ²)	0.593 \pm 0.021	0.594 \pm 0.029	0.653 \pm 0.024	0.568 \pm 0.018 ^b	0.760 \pm 0.018	0.724 \pm 0.018
Cortical bone area (mm ²)	1.12 \pm 0.04	1.00 \pm 0.03 ^b	0.926 \pm 0.025	0.799 \pm 0.033 ^a	0.968 \pm 0.028	0.854 \pm 0.018 ^a
Cortical thickness (mm)	0.307 \pm 0.006	0.266 \pm 0.007 ^d	0.243 \pm 0.004	0.225 \pm 0.009 ^c	0.241 \pm 0.006	0.220 \pm 0.003 ^b
Periosteal circumference (mm)	4.76 \pm 0.05	4.59 \pm 0.07 ^c	4.57 \pm 0.07	4.25 \pm 0.05 ^a	4.78 \pm 0.04	4.57 \pm 0.05 ^a
Endosteal circumference (mm)	2.93 \pm 0.05	2.92 \pm 0.07	3.04 \pm 0.06	2.84 \pm .004 ^a	3.27 \pm 0.04	3.19 \pm 0.04
Total BMC (mg)	2.33 \pm 0.06	1.90 \pm 0.13 ^a	1.61 \pm 0.11	1.32 \pm 0.08 ^b	1.70 \pm 0.05	1.43 \pm 0.04 ^d
Cortical BMC (mg)	1.52 \pm 0.05	1.36 \pm 0.05 ^b	1.21 \pm 0.04	1.05 \pm 0.05 ^b	1.30 \pm 0.04	1.12 \pm 0.02 ^d
Trabecular BMC (mg)	0.616 \pm 0.033	0.497 \pm 0.037 ^b	0.534 \pm 0.028	0.406 \pm 0.015 ^a	0.526 \pm 0.018	0.486 \pm 0.021
Total BMD (mg/mm ³)	597 \pm 11	535 \pm 19 ^b	491 \pm 16	459 \pm 27	477 \pm 11	429 \pm 7 ^a
Cortical BMD (mg/mm ³)	1070 \pm 32	968 \pm 10 ^b	986 \pm 16	948 \pm 21	907 \pm 11	855 \pm 6 ^d
Trabecular BMD (mg/mm ³)	362 \pm 14	289 \pm 14 ^a	302 \pm 8	262 \pm 13 ^b	275 \pm 9	252 \pm 8 ^c

^a *p* < 0.01 versus WT by two-tailed Student's *t* test.

^b *p* < 0.05 versus WT by two-tailed Student's *t* test.

^c *p* < 0.08 versus WT by two-tailed Student's *t* test.

^d *p* < 0.001 versus WT by two-tailed Student's *t* test.

Bone Phenotype of Young Adult Male *PTP-oc* Transgenic Mice—The bone phenotype of young adult male transgenic F2 progenies of all three transgenic lines was determined with pQCT (Table 1). The femur length of 10-week-old male transgenic mice of each line was slightly (by ~3%) but significantly shorter than that of corresponding age- and sex-matched WT littermates. The bone volume was also decreased by 10–15%. Similarly, total bone area, cortical bone area, cortical thickness, and periosteal circumference of femurs of these transgenic mice were significantly less than those of WT littermates. Osteoclastic *PTP-oc* transgenic expression in these male transgenic mice also reduced body weight by 6–13% compared with corresponding WT littermates.

Young adult male F2 transgenic mice of these three lines each exhibited a 16–18% decrease in total BMC and ~10% decrease in total BMD, compared with WT littermates. Trabecular BMC and BMD at the metaphysis of the distal femur each were reduced by ~20%. The reduction in BMC and BMD was not restricted to trabecular bones, since cortical BMC and BMD at middiaphysis of *PTP-oc* transgenic mice were also decreased by ~10% and 4–10%, respectively (Table 1). Because a similar bone phenotype was seen in all three lines, the observed bone loss phenotype was most probably due to targeted *PTP-oc* overexpression in osteoclastic cells and not artifacts of insertional mutation. Thus, subsequent studies were only performed with F2 progenies of transgenic line 1.

To confirm the bone loss phenotype, histomorphometry was performed at secondary spongiosa on longitudinal TRACP-stained sections of distal femurs of nine young adult male F2 transgenic mice and seven male WT littermates of transgenic line 1 (Fig. 3). Total tissue area (*T.Ar* in Fig. 3) and trabecular bone area per total tissue area (%*Tb.Ar*) of the endosteum of transgenic mice were each significantly less (by >25%) than WT controls, confirming the pQCT bone size data. The reduction in trabecular bone area per total tissue area was not due to a smaller trabecular thickness (*Tb.Th*), but due to a reduced trabecular number (*Tb.N*) (by 11%). This led to a 36% increase in trabecular separation (*Tb.Sp*). The number of TRACP+ osteoclasts per bone surface length perimeter (*NOc/BS.PM*) on

the endosteal surface was 19% greater in transgenic mice than in WT littermates. There was also a 13.5% increase in the percentage of TRACP-stained surface per bone surface length in transgenic mice compared with WT littermates (26.24 \pm 1.5 versus 23.12 \pm 1.94%; *p* = not significant), but these differences did not reach statistically significant levels due to large variations in the measurements.

To evaluate if the bone phenotype was restricted to long bones, histomorphometry was also performed on metaphyses of the L4 vertebra of 13 male F2 transgenic mice and nine male WT littermates (Fig. 4). Similar to the femoral metaphysis, targeted overexpression of *PTP-oc* in cells of osteoclastic lineage also significantly decreased trabecular perimeter (by 20%), total tissue area (by 24%), trabecular bone area per total tissue area (by 20%), and trabecular perimeter/total tissue area (by 17%) in vertebral metaphysis of young adult male transgenic mice compared with WT littermates. The increased loss of trabecular bone in the vertebra was due to a 17% decrease in trabecular number and a 35% increase in trabecular separation but not to a decrease in trabecular thickness. Overexpression of *PTP-oc* in cells of osteoclastic lineage also slightly increased number of TRACP+ osteoclasts per bone surface length (by 8%) in the vertebra. The difference was again not statistically significant, due to the relatively large variations in the measurement.

To ascertain that male transgenic progenies indeed had an elevated bone resorption, we measured the level of a serum biomarker of bone resorption (i.e. C-telopeptide of type-I collagen) in 14 male transgenic mice and compared with that in 11 age-matched male WT littermates (Fig. 5). The serum C-telopeptide level in transgenic mice was significantly higher (by >25%) than that in WT littermates, indicating that targeted overexpression of *PTP-oc* in cells of osteoclastic lineage indeed resulted in an increase in bone resorption in male transgenic mice.

To assess whether osteoclastic overexpression of *PTP-oc* would also correspondingly affect bone formation parameters *in vivo*, tetracyclines were injected into nine young adult male transgenic mice and eight age-matched male WT littermates 7 days and 1 day prior to sacrifice, respectively. Tetracycline

Effects of Osteoclastic Overexpression of PTP-oc on Blood Cell Homeostasis and on Vital Internal Organs—*PTP-oc* has been shown to have important regulatory functions in many hematopoietic cell types, such as B-lymphocytes and macrophages (7, 23). These cells also express significant levels of TRACP (4, 5, 7, 18, 24). Thus, although the TRACP exon 1C promoter is active predominantly in cells with characteristic of myeloid lineage (18), it is possible that TRACP exon 1C promoter could still be sufficiently active in these other hematopoietic cell types, resulting in an overexpression of *PTP-oc* in these blood cells. To evaluate whether the TRACP exon 1C promoter-driven *PTP-oc* overexpression in these transgenic mice would also affect blood cell homeostasis, we performed complete blood cell count analyses in 14 young adult male *PTP-oc* transgenic mice and 11 male WT littermates (Table 2). Other than a 28% ($p < 0.05$) decrease in percentage of monocytes, a borderline significant increase ($\sim 20\%$, $p = 0.061$) in total number of white blood cells, and a borderline reduction ($\sim 3\%$, $p = 0.066$) in mean corpuscular volume, there were no significant differences in any other parameters. Past studies have shown that expression of high levels of *PTP-oc* in B-lymphocytes and macrophages increased their apoptosis and reduced their proliferation *in vitro* (14, 24). That the number of total white blood cells and percentage of lymphocytes in transgenic mice not only were not decreased but rather were increased (by 21 and 8%, respectively) suggests that the use of TRACP exon 1C promoter did not lead to significant *PTP-oc* overexpression in lymphocytes and macrophages.

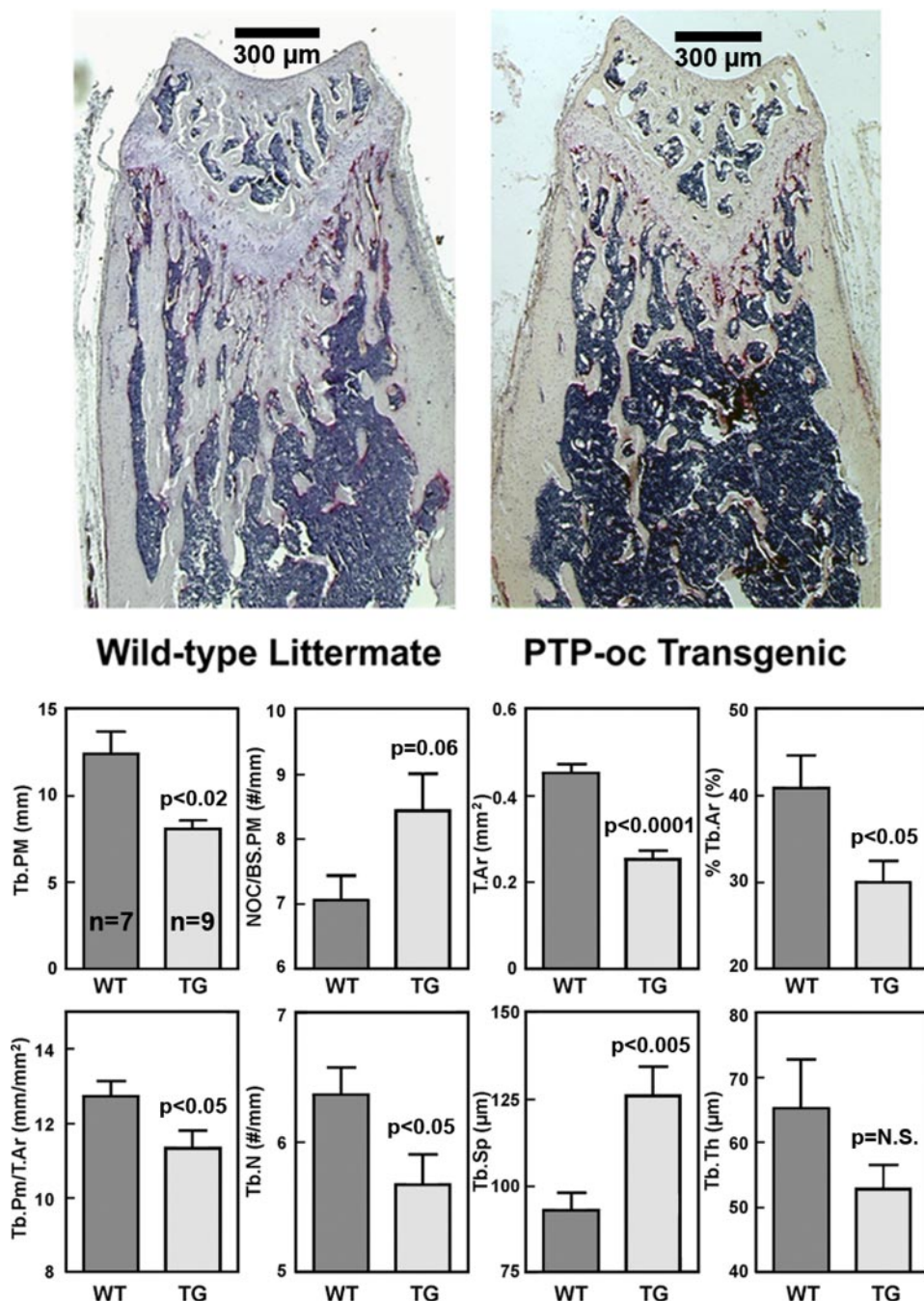


FIGURE 3. Bone histomorphometric parameters of 10-week-old male F2 transgenic and age-matched male WT littermates at the metaphysis of distal femurs. TRACP+ cells were stained in pink. Bone histomorphometry was performed at the secondary spongiosa (350 μm distal to the growth plate). The top shows a representative longitudinal section of a WT littermate and that of a transgenic mouse. Scale bars, 300 μm . The bottom summarizes the quantitative results (mean \pm S.E. of nine transgenic mice and seven WT littermates). *Tb.PM*, trabecular perimeter; *NOC/BS.PM*, number of TRACP+ osteoclasts per bone surface length; *T.Ar*, total tissue area; *Tb.Ar*, trabecular bone area per total tissue area; *Tb.N*, trabecular number; *Tb.Sp*, trabecular separation; *Tb.Th*, trabecular thickness.

labeling surfaces were measured at endosteal metaphysis of the distal femur to determine mineral apposition rate and bone formation rate. There were no statistically significant differences in tetracycline labeling surfaces, mineral apposition rate, or bone formation rate; each was not different significantly between transgenic mice and WT littermates (Fig. 6). Thus, overexpression of *PTP-oc* had little effect on dynamic bone formation parameters.

TRACP exon 1A and 1B promoters have substantial activities in several vital internal organs, including kidneys, livers, and spleens (18). As an initial step to test whether TRACP exon 1C promoter-driven *PTP-oc* overexpression might also have effects on these vital organs, we compared the weight of livers, spleens, and kidneys of 10-week-old male transgenic mice with those of age- and sex-matched WT littermates. Despite a 15% decrease in body weight, there was no significant difference in the weight of these organs (Table 3).

Transgenic Expression of PTP-oc Increased Bone Resorption in Mice

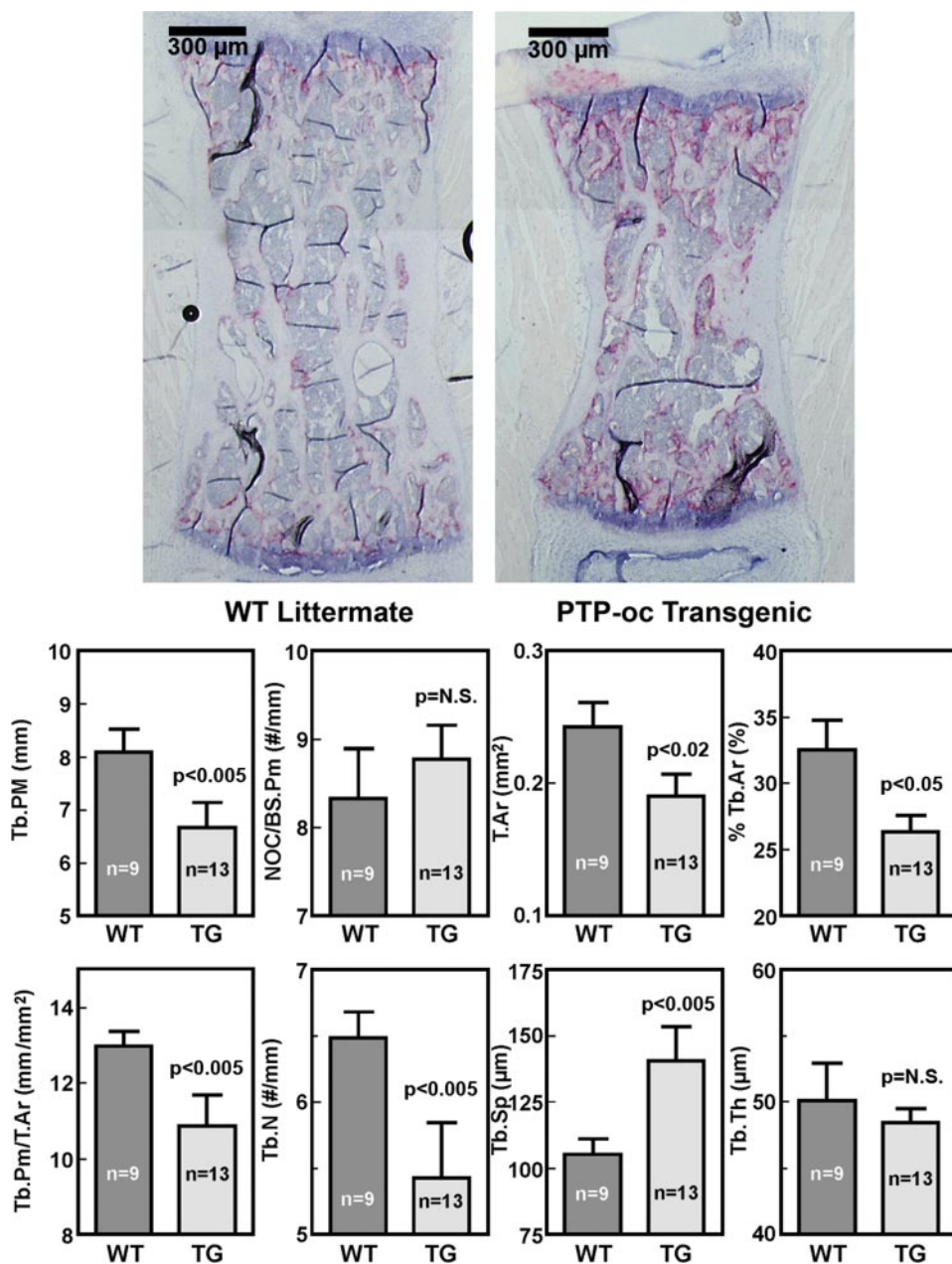


FIGURE 4. Bone histomorphometric parameters of 10-week-old male F2 transgenic and age-matched male WT littermates at the metaphysis of L4 vertebrae. TRACP+ cells were stained in pink. Measurements were performed at the bone site 350 μm away from the edge. *Top*, a representative longitudinal section of a WT littermate and that of a transgenic mouse. Scale bars, 300 μm . The *bottom* summarizes the quantitative results (mean \pm S.E. of 13 transgenic mice and nine WT mice). *Tb.PM*, trabecular perimeter; *NOC/BS.Pm*, number of TRACP+ osteoclasts per bone surface length; *T.Ar*, total tissue area; *Tb.Ar*, trabecular bone area per total tissue area; *Tb.N*, trabecular number; *Tb.Sp*, trabecular separation; *Tb.Th*, trabecular thickness.

Their adjusted weight (against body weight) was also not different between transgenic mice and WT littermates, suggesting that overexpression of *PTP-oc* with the TRACP exon 1C promoter did not appear to have significant adverse effects on these vital organs, including spleens, which expressed high *PTP-oc* levels in transgenic mice (Fig. 2B).

Absence of a Significant Bone Phenotype in Young Adult Female PTP-oc Transgenic Mice—pQCT analyses of femurs of eight 7-week-old young adult female F2 transgenic mice did not reveal a significant difference in any of the test bone parameters compared with those of 10 age-matched female WT littermates (Table 4).

The mean serum level of C-telopeptide of type-I collagen in 10 7-week-old female transgenic mice also did not differ significantly from that of 10 age-matched female WT littermates (3.02 ± 0.22 versus 2.70 ± 0.30 ng/ml, $p =$ not significant). These results indicate a sex-related discrepancy in the bone response to targeted *PTP-oc* overexpression in osteoclastic cells, leading to the lack of a readily detectable bone loss phenotype in young adult female transgenic mice.

The F2 progenies have a mixed genetic background of 75% C57BL/6J and 25% DBA2. To test the possibility that potential genetic interactions due to the mixed genetic background might have contributed to the reduced bone loss phenotype in female F2 transgenic mice, we backcrossed F2 transgenic mice with C57BL/6J mice for six generations to produce transgenic mice with >99.6% C57BL/6J background. The pQCT analyses of the femurs of 8-week-old male backcrossed transgenic mice compared with age-matched male littermates (data not shown) were similar to those shown in Table 1. The pQCT analyses of femurs of 25 8-week-old female backcrossed transgenic mice and 25 age-matched female WT littermates (Table 4) revealed that, although there were significant reductions in total BMD (by $\sim 5\%$, $p < 0.05$), trabecular BMC (by $\sim 30\%$, $p < 0.005$), and trabecular BMD (by $\sim 20\%$, $p < 0.001$) at the metaphysis of distal femur of young adult female transgenic mice compared with respective female WT littermates, the total and cortical BMC and BMD were still not different between young adult female transgenic mice and WT litter-

mates. Thus, the mixed genetic background may only partially account for the subtle bone loss phenotype in young adult female transgenic mice.

To test if the discrepancy in the bone loss phenotype between young adult male and female transgenic mice is sex hormone-related, we compared the bone parameters in five young adult female transgenic mice after 4 weeks of OVX with those in five age-matched female OVX WT mice by μ -CT (Fig. 7). There were no significant differences in the μ -CT bone parameters between the sham-operated transgenic and WT mice (data not shown), confirming the lack of

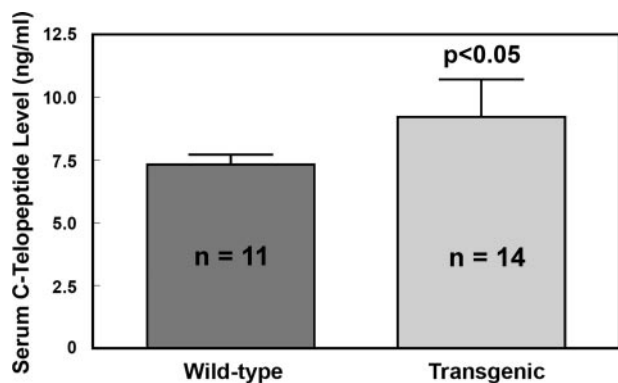


FIGURE 5. Serum levels of C-telopeptide of type I collagen of male *PTP-oc* transgenic mice (9 weeks old, $n = 14$) compared with those of age-matched male WT littermates ($n = 11$). Serum C-telopeptide levels were assayed with an enzyme-linked immunosorbant assay kit. Results are shown as mean \pm S.E.

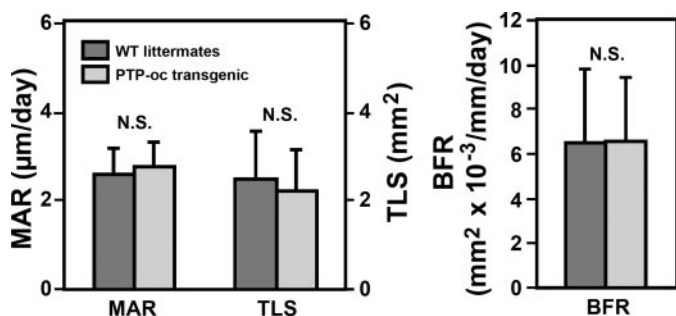


FIGURE 6. Effects of targeted overexpression of *PTP-oc* in cells of osteoclast lineage on dynamic histomorphometric bone formation parameters *in vivo*. Bone formation parameters were determined as described under "Experimental Procedures." Results are shown as mean \pm S.E. ($n = 9$ for transgenic mice and $n = 8$ for WT littermates). MAR, mineral apposition rate; TLS, tetracycline labeling surface; BFR, bone formation rate.

a detectable bone loss phenotype in young adult female transgenic mice. As expected, OVX led to significant loss of trabecular bones in both transgenic and WT mice, since there were significant reductions in trabecular bone volume (*BV* in Fig. 7), trabecular bone volume per tissue volume (*BV/TV*), and trabecular number (*Tb.N*) and a significant increase in trabecular separation (*Tb.Sp*). However, trabecular thickness (*Tb.Th*) was not affected by OVX, a finding consistent with the fact that OVX primarily increases bone resorption without a significant effect on bone formation. In contrast to trabecular bone, OVX caused only slight but insignificant reduction ($\sim 3\%$) in cortical bone volume per tissue volume (cortical *BV/TV*) at the midshaft of WT OVX littermates. On the other hand, the OVX-mediated trabecular bone loss in *PTP-oc* transgenic mice appeared to be much larger and more significant than that in age-matched WT littermates. Accordingly, there was a significantly larger reduction in trabecular separation and a borderline significant decrease in *BV/TV* in OVX transgenic mice. The decrease in cortical *BV/TV* in OVX transgenic mice was also greater ($\sim 8\%$, $p < 0.05$) than that in WT littermates. However, because of the relatively small group size ($n = 5$ for each), the differences in the other μ -CT trabecular bone parameters between transgenic and WT littermates did not reach a statistically significant level. We interpret these results to mean that the lack of a large bone loss pheno-

TABLE 2 Complete blood cell count analyses of 10-weeks old male *PTP-oc* transgenic mice and sex- and age-matched wild-type littermates (mean \pm S.E.)

Group	WBC	NE	LY	MO	EO	BA	RBC	PLT	HB	HCT	MCV	MCH	MCHC
	$10^6/\text{ml}$	%	%	%	%	%	$10^6/\text{ml}$	$10^3/\text{ml}$	g/dl	%	fL	pg/cell	g/dl
WT ($n = 11$)	7.60 ± 0.12	27.13 ± 0.33	67.80 ± 0.35	4.72 ± 0.12	0.26 ± 0.06	0.09 ± 0.02	8.02 ± 0.09	862.91 ± 1.12	11.91 ± 0.12	38.57 ± 0.28	51.41 ± 0.12	14.82 ± 0.07	28.84 ± 0.08
TG ($n = 14$)	9.19 ± 0.11	22.96 ± 0.17	73.44 ± 0.17	3.39 ± 0.07	0.15 ± 0.03	0.06 ± 0.02	8.38 ± 0.08	905.64 ± 0.81	12.29 ± 0.09	41.39 ± 0.15	49.66 ± 0.12	14.71 ± 0.67	29.67 ± 0.08
<i>p</i>	0.061	0.289	0.196	0.022	0.366	0.226	0.406	0.455	0.556	0.320	0.066	0.675	0.084

Transgenic Expression of PTP-oc Increased Bone Resorption in Mice

TABLE 3

Effects of targeted overexpression of PTP-oc in cells of osteoclastic lineage on the weight of vital organs in young adult male mice (mean \pm S.E.)

Group	Body weight	Spleens	Kidneys	Livers	Spleens/body weight	Kidneys/body weight	Livers/body weight
	<i>g</i>	<i>g</i>	<i>g</i>	<i>g</i>	%	%	%
Wild-type littermates (<i>n</i> = 8)	27.35 \pm 0.74	0.085 \pm 0.001	0.455 \pm 0.023	1.498 \pm 0.055	0.311 \pm 0.009	1.663 \pm 0.068	5.474 \pm 0.122
Transgenic mice (<i>n</i> = 8)	23.25 \pm 0.41	0.076 \pm 0.007	0.410 \pm 0.016	1.321 \pm 0.076	0.326 \pm 0.029	1.760 \pm 0.047	5.670 \pm 0.265
<i>p</i>	0.0005	0.264	0.131	0.081	0.632	0.263	0.516

TABLE 4

Comparison of bone phenotype of 8-week-old female F2 transgenic mice of transgenic line 1 (TG) with corresponding age- and sex-matched wild-type littermates (WT) (mean \pm S.E.)

	F2 mice		Backcrossed for six generations	
	WT (<i>n</i> = 11)	TG (<i>n</i> = 8)	WT (<i>n</i> = 25)	TG (<i>n</i> = 25)
Bone length (mm)	13.5 \pm 0.2	13.9 \pm 0.1	13.5 \pm 0.1	13.6 \pm 0.1
Bone volume (mm ³)	2.07 \pm 0.08	2.16 \pm 0.06	2.08 \pm 0.05	2.07 \pm 0.05
Total bone area (mm ²)	1.54 \pm 0.03	1.50 \pm 0.03	1.55 \pm 0.03	1.51 \pm 0.02
Cortical bone area (mm ²)	0.76 \pm 0.06	0.72 \pm 0.09	0.89 \pm 0.10	0.87 \pm 0.02
Cortical thickness (mm)	0.26 \pm 0.01	0.25 \pm 0.01	0.29 \pm 0.02	0.25 \pm 0.00
Periosteal circumference (mm)	4.58 \pm 0.03	4.48 \pm 0.06	4.37 \pm 0.04	4.36 \pm 0.03
Endosteal circumference (mm)	3.27 \pm 0.06	3.33 \pm 0.04	3.19 \pm 0.04	3.15 \pm 0.04
Total BMC (mg)	2.23 \pm 0.10	1.95 \pm 0.13	2.18 \pm 0.06	2.05 \pm 0.06
Cortical BMC (mg)	1.35 \pm 0.06	1.31 \pm 0.04	1.34 \pm 0.04	1.33 \pm 0.03
Trabecular BMC (mg)	0.68 \pm 0.08	0.65 \pm 0.13	0.66 \pm 0.05	0.46 \pm 0.03 ^a
Total BMD (mg/mm ³)	701.6 \pm 11.8	658.1 \pm 18.4	588.7 \pm 11.6	558.0 \pm 9.0 ^b
Cortical BMD (mg/mm ³)	993.4 \pm 53.2	1063.0 \pm 14.4	963.1 \pm 44.5	1014.7 \pm 33.0
Trabecular BMD (mg/mm ³)	320.8 \pm 26.2	289.6 \pm 43.4	314.9 \pm 15.9	246.7 \pm 9.2 ^c

^a *p* < 0.005 versus corresponding WT littermates by two-tailed Student's *t* test.

^b *p* < 0.05 versus corresponding WT littermates by two-tailed Student's *t* test.

^c *p* < 0.001 versus corresponding WT littermates by two-tailed Student's *t* test.

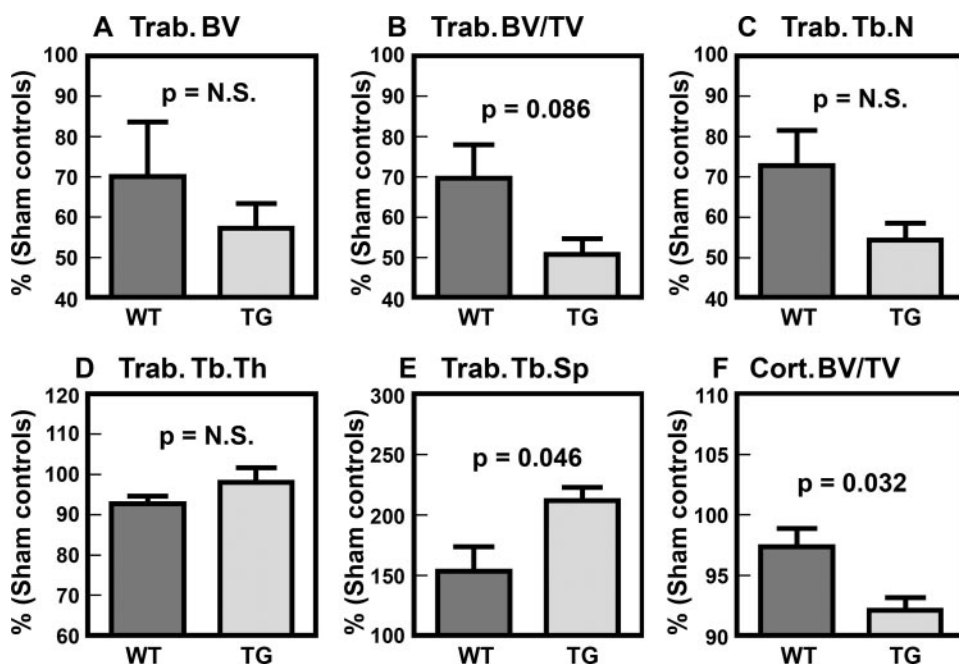


FIGURE 7. Comparison of μ -CT bone parameters of young adult OVX transgenic with those of young adult WT OVX littermates. Groups of five each of 8-week-old female PTP-oc transgenic mice and age-matched WT littermates were subjected to OVX or sham operation. Four weeks after the operation (*i.e.* at 12 weeks of age), all mice were sacrificed, and the bone parameters of right femurs were determined by μ -CT as described under "Experimental Procedures." There were no statistically significant differences (N.S.) in any of the test parameters between the sham-operated transgenic and WT mice. To more clearly show the differences in response to OVX, the results were shown as a percentage of the means of each corresponding sham-operated controls. A–E, trabecular bone parameters measured at the secondary spongiosa. F, the cortical bone volume per tissue volume parameter determined at the midshaft. Statistical significance was determined by two-tailed Student's *t* test. *Trab.*, trabecular; *Tb.N*, trabecular number; *Tb.Sp*, trabecular separation; *Tb.Th*, trabecular thickness; *Cort.*, cortical.

type in young adult female PTP-oc transgenic mice may, in part, be caused by suppressive interactions of the estrogen signaling on the PTP-oc signaling mechanism in osteoclasts.

Characterization of PTP-oc Transgenic Osteoclasts in Vitro—Western immunoblot analysis confirmed that the PTP-oc protein levels in marrow cell-derived osteoclasts of young adult male PTP-oc transgenic mice were severalfold higher than that in osteoclasts of corresponding WT littermates (Fig. 8A). The morphology of the marrow cell-derived osteoclast was also compared 7 days after treatment with 50 ng/ml sRANKL and 50 ng/ml m-CSF. The osteoclasts from the transgenic animals appeared to be larger than those derived from WT littermates (Fig. 8B). Although the number of osteoclasts formed per well was not significantly different between the two groups at concentrations of sRANKL greater than 33 ng/ml (data not shown), the average number of TRACP+, multinucleated osteoclasts formed in cultures of transgenic marrow-derived osteoclast precursor cells at low dosages of sRANKL (*i.e.* 1–10 ng/ml) was significantly greater than that in cultures of WT marrow-derived precursor cells after 7 days of cul-

ture *in vitro* (Fig. 8C). However, two-way analysis of variance reveals no significant interaction, suggesting that although PTP-oc has an enhancing effect on RANKL-mediated differen-

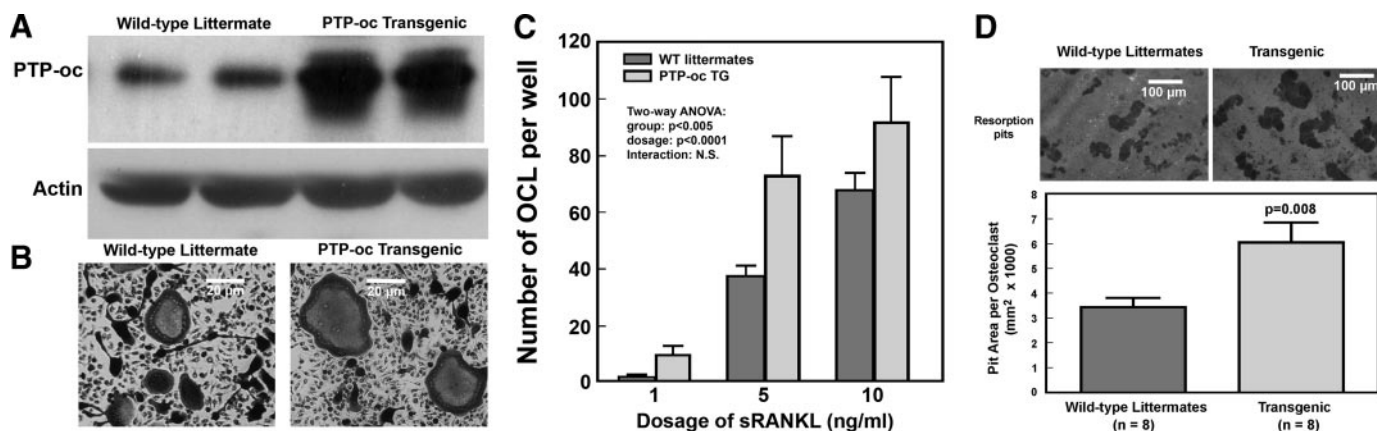


FIGURE 8. Comparison of cellular PTP-oc protein levels in marrow-derived osteoclasts (A), relative size of TRACP⁺, multinucleated osteoclasts (B), responsiveness of marrow osteoclast precursors to permissive doses of sRANKL in formation of TRACP⁺, multinucleated osteoclasts (C), and *in vitro* bone resorption activity of osteoclasts (D) of young adult male F2 transgenic mice with osteoclasts of male WT littermates. A, Western blot of the PTP-oc protein in two marrow-derived osteoclast cultures of an 8-week-old male transgenic mouse and that in two osteoclast cultures of an age-matched male WT littermates. The same blot was blotted against actin for protein loading control. B, microphotograph of a representative culture of marrow-derived osteoclasts of a 8-week-old transgenic mouse (*right*) and of an age-matched WT littermate (*left*) are shown. Scale bar, 20 μm. C summarizes the number of TRACP⁺, multinucleated osteoclasts formed from marrow-derived osteoclast precursors (at 1 × 10⁴ cells/well in 96-well plates) of 7-week-old male transgenic mice and those of age-matched male WT littermates after 7 days of treatment with 1, 5, or 10 ng/ml sRANKL and 50 ng/ml m-CSF. Results are shown as mean ± S.E. (n = 6). Statistical significance was analyzed with two-factor analysis of variance. D summarizes the *in vitro* bone resorption activity of the derived osteoclasts from eight male 10-week-old PTP-oc transgenic and eight age-matched male WT littermates on the resorption pit formation assay. Briefly, the same numbers of marrow-derived osteoclast precursors were plated on 5-mm dentine slices in a 48-well plate and were treated with RANKL and m-CSF for 7 days. The cells were then removed by sonication, and the resorption pits were stained with acid hematoxylin. The size of more than 50 resorption pits per slice was measured and divided by the number of pits to get pit area per pit (osteoclast). The *top* shows a representative field of resorption pits for each test group. Scale bar, 100 μm. The *bottom* shows the average pit area per pit (osteoclast) formed (mean ± S.E., n = 8 for each group).

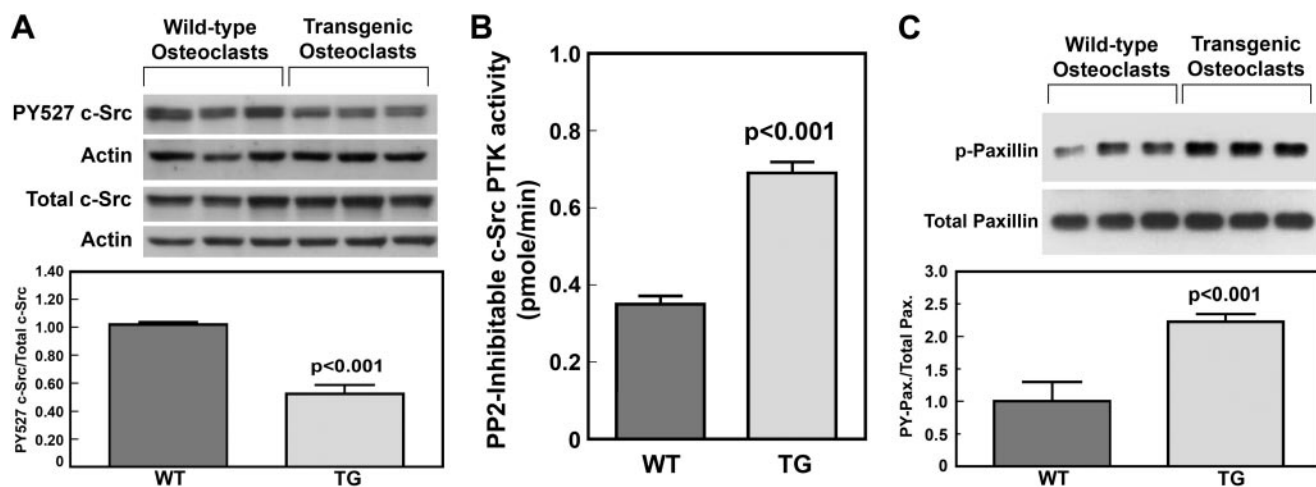


FIGURE 9. Comparison of the PY-527 levels of c-Src (A), the cellular PP2-inhibitable c-Src PTK activity (B), and protein-tyrosine-phosphorylated (PY) levels of paxillin (C) in marrow-derived osteoclasts of young adult male transgenic mice with those in osteoclasts of age- and sex-matched WT littermates. A, cell extracts of osteoclasts derived from three male transgenic mice and three WT littermates were separated on SDS-PAGE and blotted with anti-Tyr(P)⁵²⁷ c-Src and anti-actin antibodies. A replicate gel was blotted against total c-Src and actin. *Top*, Western blots. *Bottom*, ratio of PY-527 c-Src/actin to total c-Src/actin (mean ± S.E., n = 3). B, the total and PP2-inhibitable PTK activity of immunoprecipitated c-Src protein of transgenic and WT osteoclasts were assayed as described under "Experimental Procedures." Greater than 95% of the PTK activity in the immunoprecipitate was inhibited by PP2. Results are shown as PP2-inhibitable c-Src PTK activity (mean ± S.E., n = 4). C, the total and Tyr(P) levels of paxillin in osteoclast extracts of three pairs of PTP-oc transgenic mice and wild-type littermates were analyzed by the Western blot using the respective specific antibodies. *Top*, Western blots; *bottom*, ratio of protein-tyrosine phosphorylated paxillin to total paxillin (mean ± S.E., n = 3).

tiation of osteoclasts at low permissive doses of sRANKL, the enhancing effect was not of a synergistic nature. To confirm that transgenic osteoclasts were indeed more active than WT osteoclasts, the *in vitro* bone resorption activity of marrow-derived osteoclasts of eight 10-week-old male transgenic mice was compared with that of osteoclasts of eight WT littermates (Fig. 8D). The average resorption pit area/pit created by PTP-oc transgenic osteoclasts was significantly greater (~2-fold) than that created by corresponding WT osteoclasts.

Our previous *in vitro* studies have suggested that PTP-oc stimulates the overall bone resorption activity of osteoclastic cells in part through activation of the c-Src PTK activity via dephosphorylation of Tyr(P)⁵²⁷ (13–16). Consistent with our previous findings, the relative Tyr(P)⁵²⁷ c-Src to total c-Src levels in marrow-derived osteoclasts of young adult male transgenic mice were ~50% that of those in osteoclasts of age-matched male WT littermates (Fig. 9A). Fig. 9B shows that the PP2-inhibitable PTK activity of the immunoprecipitated c-Src

Transgenic Expression of PTP-oc Increased Bone Resorption in Mice

protein of transgenic osteoclasts was also ~2-fold greater than that of WT osteoclasts. This was due to an increase in PTK activity and not to an increase in c-Src protein, because there were no significant differences in cellular c-Src protein levels between transgenic and WT osteoclasts. Further consistent with the premise that the c-Src PTK activity is more active in transgenic osteoclasts than in WT osteoclasts, the protein-tyrosine phosphorylated levels of paxillin (a substrate of c-Src PTK in osteoclasts (25)) in transgenic osteoclasts were also about twice as high as those in WT osteoclasts (Fig. 9C).

DISCUSSION

Although our previous studies have afforded strong *in vitro* evidence that PTP-oc is a positive regulator of osteoclast activity and that its enhancing action is mediated in part through activation of the PTK activity of c-Src via the PTP-oc-mediated dephosphorylation of its Tyr(P)⁵²⁷ residue (13–16), there had been no *in vivo* evidence supporting the contention that PTP-oc is an important regulator of osteoclastic resorption until now. Accordingly, this report has clearly demonstrated that young adult male transgenic mice with targeted *PTP-oc* overexpression in cells of osteoclastic lineage (generated with the TRACP exon 1C promoter, which is specific for osteoclastic cells) exhibited significant reductions in bone mass and density *in vivo*. Thus, there is now strong evidence supporting the importance of PTP-oc *in vivo*. Importantly, these male transgenic mice exhibited a highly significant increase in the level of C-telopeptide of type I collagen and were without significant changes in the histomorphometric bone formation parameters, when compared with sex- and age-matched WT littermates. These results would indicate that the bone loss was due solely to an increase in osteoclastic resorption and not to a decrease in bone formation. Our *in vitro* findings that the average size of resorption pits created by marrow-derived osteoclasts of young adult male *PTP-oc* transgenic mice was twice as large as those created by marrow-derived osteoclasts of WT littermates provide additional support for the conclusion that targeted overexpression of *PTP-oc* in cells of osteoclastic lineage leads to an increase in bone resorption activity of the mature osteoclast.

Most overexpression transgenic mouse studies employed powerful promoters to drive expression of the transgene, which typically yielded tens (and often hundreds)-fold increases in transgene expression. In contrast, the average -fold expression level of the rabbit *PTP-oc* transgene in marrow-derived osteoclasts of our transgenic mice was relatively low (*i.e.* on the average, ~4-fold of that of endogenous murine *PTP-oc* mRNA). This relatively low level of overexpression of *PTP-oc*, which was most probably due to the use of the weak TRACP exon 1C promoter (19) to drive transgene expression, is noteworthy in two respects. First, the relatively low levels of PTP-oc transgenic expression might minimize the risk for off-target effects, which can be caused by sequestration or trapping of nonphysiological substrates or binding partners due to the very high level of transgene expression in target cells. Second, the fact that substantial increases in resorption activity of mature osteoclasts can be seen with only an average 4-fold increase in *PTP-oc* overexpression, *in vivo*, may have physiological implications. In this regard, we have previously shown that treat-

ment of primary rabbit osteoclasts with resorption activators resulted in 2–3-fold up-regulations of PTP-oc expression *in vitro* (16), suggesting that the observed 4–5-fold *PTP-oc* up-regulation in osteoclasts is attainable under physiologically relevant situations. Consequently, we conclude that PTP-oc indeed functions as a positive regulator of osteoclasts *in vivo* to increase their bone resorption activity.

There is *in vitro* evidence that overexpression of *PTP-oc* could lead to suppression of the proliferation and/or enhancement of apoptosis in B-lymphocytes and macrophages (5, 7, 14, 24). However, this study shows that transgenic overexpression of *PTP-oc* using the TRACP exon 1C promoter did not significantly reduce the total number of white blood cells or the percentage of lymphocytes in transgenic mice. There is also no compelling evidence that TRACP exon 1C promoter-directed *PTP-oc* overexpression would adversely affect blood cell homeostasis in our transgenic mice. Although we did not measure the expression level of *PTP-oc* in blood cells other than marrow-derived osteoclasts of transgenic mice, these findings suggest that use of the TRACP exon 1C promoter to drive *PTP-oc* expression did not lead to substantial overexpression of *PTP-oc* in B-lymphocytes and/or macrophages *in vivo* that would result in suppression of proliferation and/or increased apoptosis of these cells. This speculation is consistent with the previous conclusion that the TRACP exon 1C promoter is specific for myeloid cells and is only modestly active in macrophages or lymphocytes (18). On the other hand, there was a significant 28% decrease in the percentage of monocytes, raising the possibility that overexpression of *PTP-oc* in precursor cells of the monocyte/osteoclast lineage might have favored osteoclastic over monocytic differentiation.

An intriguing observation of this study is the discrepancy in the bone loss phenotype between young adult male and female transgenic mice compared with respective WT littermate controls. Accordingly, although the bone loss and osteoclastic resorption phenotype was readily observed in young adult male F2 transgenic mice, it was much more subtle in young adult female F2 transgenic mice. Understanding the underlying mechanisms for such sex-related discrepancy in the bone loss phenotype of these *PTP-oc* transgenic mice would not only provide insight into the molecular mechanism of *PTP-oc* in regulating osteoclast activity but could also have clinical implications with respect to potential roles of *PTP-oc* in pathophysiology of postmenopausal osteoporosis.

The mechanism leading to the subtle bone loss phenotype in female *PTP-oc* transgenic mice is likely to be complex. Because the phenotype of the female transgenics was more apparent when the line was backcrossed to the C57BL/6J strain and the variation in the genetic background was reduced, the failure to detect a phenotype in the initial study of the females may have been partly due to a mixed genetic background. However, the phenotype was still only apparent in trabecular bone, suggesting that other mechanisms were also responsible. Because estrogen is the sex hormone that largely determines sex-related characteristics in females and because the estrogen receptor α (ER α) signaling is shown to have a pivotal role in the estrogen-mediated suppression of bone loss in female but not male mice (26), it is conceivable that interactions between the PTP-oc sig-

naling and that of the ER α could contribute to the apparent discrepancy in the bone resorption response to osteoclastic overexpression of *PTP-oc* between young adult female and male transgenic mice. Our findings that the trabecular and cortical bone loss phenotype in young adult female transgenic mice was enhanced significantly by OVX compared with that in corresponding WT OVX controls support our speculation that there may be suppressive interaction of estrogen on the PTP-oc signaling in female transgenic mice. The exact nature of such putative interaction is unclear. Determination of such an interaction would require a better understanding of the molecular mechanism(s) by which the ER α signaling mediates the estrogen-dependent suppression of bone loss in female but not male mice (26). However, it is interesting to note that the sex-related discrepancy in the bone phenotype is not unique to *PTP-oc* transgenic mice, since it has also been reported in *PTP- ϵ* knock-out mice (27). However, in contrast to our results in the PTP-oc transgenic mice, the observed increased trabecular bone mass phenotype in *PTP- ϵ* -deficient mutant mice was most prevalent in young adult females (27). Like PTP-oc, PTP- ϵ appears to be a positive regulator of osteoclast activity (27). The observation that genetic manipulation of expression of these two distinct PTPs that have been shown to be positive regulators of osteoclast activity would each yield sex-related discrepancies in the osteoclastic resorption phenotype is interesting. It raises the possibility of significant similarities between the signaling mechanism of PTP-oc and that of PTP- ϵ signaling with respect to their potential interactions with the ER α signaling in osteoclasts. This has clinical ramifications, since understanding the interaction between signaling mechanisms of these PTPs and ER α in osteoclasts not only could offer insights into the pathophysiology of postmenopausal osteoporosis but may also open up a new avenue of research that may eventually lead to development of novel therapeutic modalities for bone wasting diseases.

The precise molecular mechanism(s) by which PTP-oc acts to stimulate the bone resorption activity of mature osteoclasts *in vivo* remains to be determined. Our previous *in vitro* studies have indicated that the molecular mechanism by which PTP-oc regulates the bone resorption activity of mature osteoclasts may, in part, involve activation of the c-Src PTK activity through dephosphorylation of the inhibitory Tyr(P)⁵²⁷ residue of c-Src (13–16). We recently found that the steady state Tyr(P)⁵²⁷ phosphorylation level of c-Src in marrow-derived osteoclasts of young adult male transgenic mice was 50% lower than that in marrow-derived osteoclasts of corresponding WT littermates, a finding that is consistent with our contention that PTP-oc acts as a c-Src Tyr(P)⁵²⁷ PTP in osteoclasts (15). The ~2-fold increase in the PP2-inhibitable c-Src PTK activity and the steady state protein-tyrosine phosphorylation level of paxillin, a known cellular substrate of c-Src in osteoclasts (25), in marrow-derived osteoclasts of young adult transgenic mice compared with corresponding WT osteoclasts are also consistent with the premise that the *PTP-oc* overexpression-dependent decreases in c-Src Tyr(P)⁵²⁷ phosphorylation are associated with an activation of its PTK activity and its signaling transduction. Therefore, these results provided strong circumstantial

evidence for our premise that PTP-oc regulates osteoclast activity *in vivo* in part through activation of the PTK activity and the signal transduction mechanism of c-Src in osteoclasts (13–16). Although the molecular mechanism by which the PTP-oc-mediated c-Src activation promotes osteoclastic resorption has not been clearly established, our previous *in vitro* studies have indicated that one of the consequences of the PTP-oc-mediated activation of the c-Src signaling in osteoclastic cells is to promote osteoclast survival, in part, through c-Src-dependent activation of NF κ B and JNK2 (15), which we believe would in part lead to an increase in the overall bone resorption activity of the mature osteoclast.

Under normal physiological conditions, bone formation is tightly coupled to resorption during remodeling, in that an increase in bone resorption is followed by a compensatory increase in bone formation. Intriguingly, despite the relatively large increases in bone resorption in our *PTP-oc* transgenic mice, there was no evidence for any coupled effects of *PTP-oc* overexpression on bone formation in these transgenic mice. The lack of corresponding increases in the compensatory bone formation implies a defective bone coupling in these *PTP-oc* transgenic mice. The underlying mechanistic reason for the apparent uncoupling of bone formation to the increased bone resorption is unclear. Defective bone coupling has been implicated as a key contributing factor for bone loss in many metabolic bone diseases with excessive bone resorption, such as postmenopausal osteoporosis (28), hyperparathyroidism (29), hyperthyroidism (29), renal insufficiency (30), and osteodystrophies (31). It is conceivable that pathologic conditions with persistent activation of bone resorption (such as in the case of *PTP-oc* overexpression) could create a situation where a “disequilibrium” develops between resorption and the coupled bone formation. The precise molecular mechanism linking the coupled bone formation to resorption has not been clearly delineated, but there is substantial evidence that one or more locally produced “coupling factors” may be involved (32). Although the nature and cellular source of such local “coupling factors” have not been determined, one of the concepts postulates that coupling is accomplished through the release of bone matrix growth factors, such as insulin-like growth factors (33) or TGF β (34), during the bone resorption process to stimulate bone formation. More recently, Martin and Sims (35) have also advanced an alternative concept, suggesting that the activated osteoclast, rather than bone matrix, is the source of the putative “coupling factors.” However, our findings that *PTP-oc* transgenic mice exhibited a relatively large increase in bone resorption activity (presumably due to the increased number of activated osteoclasts) without corresponding increases in bone formation are not entirely compatible with either concept. Thus, the molecular process coupling bone formation to the increased resorption is likely to be highly complex and involve multiple mechanisms. It is interesting to note that ablation of c-Src (one of the presumed downstream mediators of PTP-oc) in mice also resulted in dissociation between bone resorption and the coupled bone formation in that c-Src deficiency completely suppressed bone resorption without an effect on bone formation (36). In addition, suppression of bone resorption through abrogation of expression or activity of chloride chan-

Transgenic Expression of PTP-oc Increased Bone Resorption in Mice

nel CLCN7 (37) also showed no corresponding suppression of bone formation. The significance of these observations as well as our findings of the uncoupling of bone formation from resorption remains unclear.

It should also be noted that the uncoupling of bone formation from resorption has also been reported in transgenic mice deficient in two other PTP activities that have shown to regulate osteoclast activity. Accordingly, motheaten mice, deficient in functional SHP-1, not only exhibited enhanced bone resorption (due to the increased formation of overactive osteoclasts) but also showed a defective coupling mechanism (38, 39). Mice deficient in *PTP-ε* also exhibited a drastic reduction in osteoclastic resorption without significant changes in bone formation (27). Thus, we cannot rule out the intriguing possibilities that protein-tyrosine phosphorylation reactions may play some essential roles in the bone coupling process and that those PTPs that are involved in regulation of osteoclast activity, including PTP-oc, may play regulatory roles in the bone coupling mechanism.

Finally, this study also provided circumstantial evidence that PTP-oc may have a regulatory role in osteoclast differentiation *in vivo*. Specifically, our histomorphometric analyses revealed that targeted overexpression of PTP-oc in cells of osteoclast lineage also increased the percentage of TRACP-stained surface per bone surface length and the number of TRACP+ osteoclasts per bone surface. Although these differences barely missed the statistically significant levels due to the large variations in the measurements, these findings raise the possibility that *PTP-oc* overexpression may also increase the number of active osteoclasts per bone surface *in vivo* in addition to increasing their bone resorption activity. That *PTP-oc* overexpression appeared to enhance the response of osteoclast precursors to low (but not high) dosages of sRANKL in differentiation of TRACP+, multinucleated osteoclasts, *in vitro*, further supports a regulatory role of PTP-oc in RANKL-mediated osteoclast differentiation. This tentative conclusion is in agreement with our previous *in vitro* observations that overexpression of WT-*PTP-oc* increased, whereas overexpression of phosphatase-deficient *PTP-oc* or suppression of *PTP-oc* expression by small interfering RNA reduced, the RANKL-mediated formation of osteoclast-like cells from the preosteoclastic human U937 or murine RAW264.7 cells (14, 15). Moreover, our recent demonstration that targeted deletion of the PTP-oc intronic promoter *in vitro* completely prevented sRANKL-mediated osteoclastic differentiation of RAW264.7 cells (40) also implicates an important regulatory role of PTP-oc in the RANKL-mediated osteoclast differentiation. The molecular mechanism of PTP-oc stimulating differentiation of osteoclast precursors remains elusive. Because c-Src PTK is not likely to be involved in osteoclast differentiation (41, 42), PTP-oc most probably acts through c-Src-independent pathways to promote differentiation of osteoclast precursors. Deficient *PTP-oc* expression did not affect the expression levels of *c-fos*, *mitf*, and *Pu.1* (transcription factors that are known to be involved in the RANKL-mediated osteoclast differentiation) or *RANK* (40). Thus, these transcription factors may not be involved in the PTP-oc-induced RANKL-dependent osteoclastic differentiation of RAW264.7 cells. However, these findings did not preclude the

possibility that the PTP-oc signaling acts as a downstream mediator of these transcription factors. It is also not possible at this time to determine if *PTP-oc* overexpression acts principally on enhancing osteoclastic activity and/or also on increasing osteoclast numbers to increase bone resorption.

In summary, this study has demonstrated that targeted transgenic overexpression of *PTP-oc* with TRACP 1C exon promoter in cells of osteoclastic lineage led to a marked reduction in trabecular bone mass in male but not female young adult transgenic mice. This was due to an increase in the bone resorption activity of mature osteoclasts. These findings provide the first compelling evidence that PTP-oc is a positive regulator of osteoclastic activity *in vivo*.

Acknowledgments—This work was performed in facilities provided by the Department of Veterans Affairs. We express appreciation and gratitude to Dr. A. Ian Cassady for generously providing the pGL3-TRACP-1C-Luc expression plasmid. We also acknowledge the excellent technical assistance of Anil Kapoor in performing μ -CT analyses.

REFERENCES

1. Miyazaki, T., Tanaka, S., Sanjay, A., and Baron, R. (2006) *Mod. Rheumatol.* **16**, 68–74
2. Ross, F. P., and Teitelbaum, S. L. (2005) *Immunol. Rev.* **208**, 88–105
3. Xiong, W. C., and Feng, X. (2003) *Front. Biosci.* **8**, d1219–d1226
4. Wu, L.-W., Baylink, D. J., and Lau, K.-H. W. (1996) *Biochem. J.* **316**, 515–523
5. Seimiya, H., Sawabe, T., Inazawa, J., and Tsuruo, T. (1995) *Oncogene* **10**, 1731–1738
6. Wiggins, R. C., Wiggins, J. E., Goyal, M., Wharram, B. L., and Thomas, P. E. (1995) *Genomics* **27**, 174–181
7. Aguiar, R. C. T., Yakushijin, Y., Kharbanda, S., Tiwari, S., Freeman, G. J., and Shipp, M. A. (1999) *Blood* **94**, 2403–2413
8. Andersen, J. N., Jansen, P. G., Echwald, S. M., Mortensen, P. H., Fukada, T., Del Vecchio, R., Tonks, N. K., and Møller, N. P. (2004) *FASEB J.* **18**, 8–30
9. Bischof, J. M., and Wevrick, R. (2005) *Physiol. Genomics* **22**, 191–196
10. Amoui, M., Baylink, D. J., Tillman, J. B., and Lau, K.-H. W. (2003) *J. Biol. Chem.* **278**, 44273–44280
11. Jacob, S. T., and Motiwala, T. (2005) *Cancer Gene Ther.* **12**, 665–672
12. Yang, J. H., Amoui, M., Strong, D. D., and Lau, K.-H. W. (2007) *Arch. Biochem. Biophys.* **465**, 72–81
13. Suhr, S. M., Pamula, S., Baylink, D. J., and Lau, K.-H. W. (2001) *J. Bone Miner. Res.* **16**, 1795–1803
14. Amoui, M., Suhr, S. M., Baylink, D. J., and Lau, K.-H. W. (2004) *Am. J. Physiol.* **287**, C874–C884
15. Amoui, M., Sheng, M. H.-C., Chen, S. T., Baylink, D. J., and Lau, K.-H. W. (2007) *Arch. Biochem. Biophys.* **463**, 47–59
16. Lau, K.-H. W., Wu, L.-W., Sheng, M. H.-C., Amoui, M., Suhr, S. M., and Baylink, D. J. (2006) *J. Cell. Biochem.* **97**, 940–955
17. Wharram, B. L., Goyal, M., Gillespie, P. J., Wiggins, J. E., Kershaw, D. B., Holzman, L. B., Dysko, R. C., Saunders, T. L., Samuelson, L. C., and Wiggins, R. C. (2000) *J. Clin. Invest.* **106**, 1281–1290
18. Walsh, N. C., Cahill, M., Carninci, P., Kawai, J., Okazaki, Y., Hayashizaki, Y., Hume, D. A., and Cassady, A. I. (2003) *Gene (Amst.)* **307**, 111–123
19. Pan, W., Mathews, W., Donohue, J. M., Ramnaraine, M. L., Lynch, C., Selski, D. J., Walsh, N., Cassady, A. I., and Clohisy, D. R. (2005) *J. Biol. Chem.* **280**, 4888–4893
20. Wergedal, J. E., Sheng, M. H.-C., Ackert-Bicknell, C. L., Beamer, W. G., and Baylink, D. J. (2005) *Bone* **36**, 111–122
21. Sheng, M. H.-C., Baylink, D. J., Beamer, W. G., Donahue, L. R., Lau, K.-H. W., and Wergedal, J. E. (2002) *Bone* **30**, 486–491
22. Srivastava, A. K., Bhattacharyya, S., Li, X., Mohan, S., and Baylink, D. J. (2001) *Bone* **29**, 361–367
23. Rundle, C. H., Strong, D. D., Chen, S.-T., Linkhart, T. A., Sheng, M.-H. C.,

Transgenic Expression of PTP-oc Increased Bone Resorption in Mice

- Wergedal, J. E., Lau, K.-H. W., and Baylink, D. J. (2008) *J. Gene Med.* **10**, 229–241
24. Seimiya, H., and Tsuruo, T. (1998) *J. Biol. Chem.* **273**, 21187–21193
25. Zhang, Z., Baron, R., and Horne, W. C. (2000) *J. Biol. Chem.* **275**, 37219–37223
26. Nakamura, T., Imai, Y., Matsumoto, T., Sato, S., Takeuchi, K., Igarashi, K., Harada, Y., Azuma, Y., Krust, A., Yamamoto, Y., Nishina, H., Takeda, S., Takayanagi, H., Metzger, D., Kanno, J., Takaoka, K., Martin, T. J., Chambon, P., and Kato, S. (2007) *Cell* **130**, 811–823
27. Chiusaroli, R., Knobler, H., Luxenburg, S., Sanjay, A., Granot-Attas, S., Tiran, Z., Miyazaki, T., Harmelin, A., Baron, R., and Elson, A. (2004) *Mol. Biol. Cell* **15**, 234–244
28. Ivey, J. L., and Baylink, D. J. (1981) *Metab. Bone Dis. Relat. Res.* **3**, 3–7
29. Parisien, M., Silverberg, S. J., Shane, E., Dempster, D. W., and Bilezikian, J. P. (1990) *Endocrinol. Metab. Clin. N. Am.* **19**, 19–34
30. Mosekilde, L., and Melsen, F. (1978) *Acta Med. Scand.* **204**, 97–102
31. Kraut, J. A. (1995) *Adv. Ren. Replace. Ther.* **2**, 40–51
32. Howard, G. A., Bottemiller, B. L., Turner, R. T., Rader, J. I., and Baylink, D. J. (1981) *Proc. Natl. Acad. Sci. U. S. A.* **78**, 3204–3208
33. Mohan, S., and Baylink, D. J. (1996) *Horm. Res.* **45**, Suppl. 1, 59–62
34. Pivonka, P., Zimak, J., Smith, D. W., Gardiner, B. S., Dunstan, C. R., Sims, N. A., Martin, T. J., and Mundy, G. R. (2008) *Bone* **43**, 249–263
35. Martin, T. J., and Sims, N. A. (2005) *Trends Mol. Med.* **11**, 76–81
36. Marzia, M., Sims, N. A., Voit, S., Migliaccio, S., Taranta, A., Bernardini, S., Faraggiana, T., Yoneda, T., Mundy, G. R., Boyce, B. F., Baron, R., and Teti, A. (2000) *J. Cell Biol.* **151**, 311–320
37. Schaller, S., Henriksen, K., Sveigaard, C., Heegaard, A. M., Hélix, N., Stahlhut, M., Ovejero, M. C., Johansen, J. V., Solberg, H., Andersen, T. L., Hougaard, D., Berryman, M., Shiødt, C. B., Sørensen, B. H., Lichtenberg, J., Christophersen, P., Foged, N. T., Delaissé, J. M., Engsig, M. T., and Karsdal, M. A. (2004) *J. Bone Miner. Res.* **19**, 1144–1153
38. Umeda, S., Beamer, W. G., Takagi, K., Naito, M., Hayashi, S., Yonemitsu, H., Yi, T., and Shultz, L. D. (1999) *Am. J. Pathol.* **155**, 223–233
39. Aoki, K., Didomenico, E., Sims, N. A., Mukhopadhyay, K., Neff, L., Houghton, A., Amling, M., Levy, J. B., Horne, W. C., and Baron, R. (1999) *Bone* **25**, 261–267
40. Yang, J. H., Amoui, M., and Lau, K.-H. W. (2007) *FEBS Lett.* **581**, 2503–2508
41. Soriano, P., Montgomery, C., Geske, R., and Bradley, A. (1991) *Cell* **64**, 693–702
42. Xing, L., Venegas, A. M., Chen, A., Garrett-Beal, L., Boyce, B. F., Varmus, H. E., and Schwartzberg, P. L. (2001) *Genes Dev.* **15**, 241–253
43. Sheng, M. H.-C., Amoui, M., Stiffel, V., Srivastava, A. K., Wergedal, J. E., and Lau, K.-H. W., *Meeting of the American Society of Bone and Mineral Research, Honolulu, HI, September 2007*, Abstr. O112